Carbohydrate Polymers 216 (2019) 270–281

Contents lists available at ScienceDirect

Carbohydrate Polymers

journal homepage: www.elsevier.com/locate/carbpol

Structural elucidation, antioxidant and immunomodulatory activities of a novel heteropolysaccharide from cultured *Paecilomyces cicadae* (Miquel.) Samson

Yanbin Wang[a], Pengfei He[b], Liang He[a,*], Qingrong Huang[d], Junwen Cheng[a], Weiqi Li[c], Yu Liu[c], Chaoyang Wei[c]

[a] Key Laboratory of State Forest Food Resources Utilization and Quality Control, Zhejiang Provincial Key Laboratory of Forest Food, Zhejiang Academy of Forestry, Hangzhou 310023, China
[b] Department of Processing, Marine Fisheries Research Institute of Zhejiang, Zhoushan 316021, China
[c] Institute of Biochemistry, College of Life Sciences, Zhejiang University, Hangzhou 310058, China
[d] Department of Food Science, Rutgers University, 65 Dudley Road, New Brunswick, NJ 08901, USA

ARTICLE INFO

Keywords:
Paecilomyces cicadae
Heteropolysaccharide
Structural elucidation
Biological activity
AFM

ABSTRACT

The fine structure and chain conformation of a heteropolysaccharide (PCIPS3) from mycelium of *Paecilomyces cicadae* were investigated *via* the analysis of HPLC, IR, methylation, NMR spectroscopy and multiangle light scattering. It was determined to be a 2.23×10^4 g/mol heteropolysaccharide primarily composed of glucose, galactose and mannose in a molar ratio of 23.8:2.1:1.0. The PCIPS3 backbone consisted of 1,4-linked α-D-Glc*p* and 1,4-linked 6-*O*-Me-α-D-Glc*p* residues, which were occasionally interrupted by branched β-Gal*f* residues through 1,6-linkage. Moreover, the α (0.60) from Mark–Houwink–Sakurada (MHS) equation suggested that PCIPS3 adopted a flexible chain conformation in 0.1 mol/L $NaNO_3$ at 25 °C. The worm-like chains model parameters for PCIPS3 were estimated as following: $M_L = 437\ nm^{-1}$, $q = 0.46$ nm and 0.79 nm, which were further evidenced by AFM. Furthermore, PCIPS3 showed excellent scavenging capacities of 2,2-diphenyl-1-picrylhydrazyl radical, superoxide radical, hydroxyl radical, ORAC radical and moderate immunomodulatory activity.

1. Introduction

Cordyceps cicadae Shing (called "Chan Hua" in Chinese), which belongs to the Ascomycota, Hypocreales, Claviceptaceae, Cordeceps, and parasites on the larvae of *Cicada flammata* Dist, is a valued Chinese caterpillar fungus that has been extensively used as tonic food and medicine for a long time (Sun et al., 2017). It has attracted considerable attention due to its wide-range of nutritional and pharmacological benefits on the immune, circulatory, cardiovascular, hematogenic and respiratory systems (Ke & Lee, 2018; Weng, Chou, Lin, Wsai, & Kuo, 2002). However, the natural recalcitrance of Cordyceps slows down its commercialization, including the specific host, the strictly conditioned environment and artificial destruction.

Paecilomyces cicadae (Miquel) Samson is thought to be the anamorph stage of Cordyceps. Culture of this entomogenous fungi in submerged fermentation has become a promising way to meet the needs of human consumption. More and more secondary metabolites have been discovered from the artificial culture and mycelium including polysaccharides, cordycepic acid, ergosterol peroxide and effective nucleosides (Chai et al., 2007; Shen et al., 2007; Xiao et al., 2004). For human beings, these secondary metabolites can be developed to be biofunctional agents with amazing potential in improving health and preventing diseases. Among them, some hetero-polysaccharides derived from *P. cicadae* have attracted great attention due to their intriguing biological activities, including anti-tumor (Shen et al., 2007; Sun et al., 2017), immunomodulation (Cheng et al., 2012; Xu et al., 2018), anti-inflammation (Ke & Lee, 2018), anti-bacteria (Zhang et al., 2017) and anti-oxidation (He, Wu, Cheng, Li, & Lu, 2010; Ren, He, Cheng, & Chang, 2014).

Many studies have been reported that the biological activities of polysaccharides are not only dependent on their chemical structures, but also closely related to their unique architectures, especially the advanced helical conformations (Yang & Zhang, 2009). Therefore, it is interesting and essential to elucidate the role of chemical features and

* Corresponding author.
E-mail address: kite006@126.com (L. He).

https://doi.org/10.1016/j.carbpol.2019.03.104
Received 25 December 2018; Received in revised form 29 March 2019; Accepted 30 March 2019
Available online 07 April 2019
0144-8617/

chain conformations of polysaccharides on their biological activities (Hu et al., 2017; Ding, Qian, Goff, Wang, & Cui, 2018). In our previous research (Cheng et al., 2012; Wei, Li, Shao, He, & Cheng, 2016), crude polysaccharides obtained from the mycelium of *P. cicadae* has been fractionated into three sub-fractions, namely PCIPS1, PCIPS2 and PCIPS3. Further, the fine structure and chain conformation of heteromannan (PCIPS2) has been characterized, which might shed light on its immuno-stimulating activity on murine macrophage RAW264.7 proliferative response. Unfortunately, other fractions still need definitive evidence to develop this kind of fermented resources.

Therefore, in order to obtain a comprehensive knowledge of the polysaccharides from the mycelium of *P. cicadae*, we further purified the third fraction (PCIPS3) and characterized its chemical structure and advanced architecture by monosaccharide composition, Fourier transform infrared spectroscopy (FT-IR), methylation, 1D/2D nuclear magnetic resonance (NMR), size exclusion chromatography combined with multiangle laser light scattering. Moreover, its antioxidant activities were detected by different assays for better understanding the relationship of the structure-function.

2. Materials and methods

2.1. Materials and reagents

The strain of *P. cicadae* ZJ001 was screened and collected from Zhejiang Academy of Forestry, Hangzhou city, Zhejiang Province, China. And it was maintained on potato dextrose agar (PDA) slant subcultured every 4 weeks. According to our previous report (Cheng et al., 2012; Wei et al., 2016), the crude polysaccharide was extracted from the mycelia of *P. cicadae* with distilled water at 80 °C and precipitated with 75% ethanol. The fractionation of PCIPS3 was collected after DEAE-Sepharose Fast Flow chromatography.

Dextran standard (Mw = 41 400 Da) was obtained from American Polymers Standards Co. (Mentor, OH, USA). The compounds 1,1-diphenyl-2-picrylhydrazyl radical 2,2-diphenyl-1-(2,4,6-trinitrophenyl) hydroxyl (DPPH), 6-hydroxy-2,5,7,8-tetramethylchroman-2-carboxylic acid (Trolox), 2,2′-azobis(2-amidinopropane) dihydrochloride (AAPH), nicotinamide adenine dinucleotide (NADH), nitroblue tetrazolium (NBT), potassium ferricyanide and lipopolysaccharide (LPS) were purchased from Sigma Chemical Co. (St. Louis, MO, USA). Deuterium oxide (99.9%) was from J&K Scientific Ltd (Beijing, China). Ultrapure water was produced by Milli-Q system (Millipore, Billerica, USA). All other reagents were of analytical grade and purchased from local chemical suppliers in China.

2.2. General analysis of PCIPS3 from cultured P. cicadae

PCIPS3 (10 mg/mL) was initially loaded onto a Sephadex G-100 gel column (1.6 cm × 80 cm) and then purified on a Sephadex G-75 gel column (1.6 cm × 80 cm), which was both eluted by 0.05 mol/L PBS containing 0.1 mol/L NaCl (pH 7.0) at a flow rate of 0.5 mL/min. The eluate (3 mL/tube) was collected with a fraction collector, dialyzed against distilled water for 48 h and finally freeze-dried to afford the purified product.

The total sugar content was determined by phenol-sulphuric acid method using glucose as standard (Dubois, Gilles, Hamilton, Rebers, & Smith, 1956). The protein content was evaluated with the Bradford method, using bovine serum albumin as the standard (Bradford, 1976). The uronic acid content was determined by photometry with m-hydroxybiphenyl at 525 nm using D-galacturonic acid as the standard (Blumenkrantz & Asboe-Hansen, 1973).

2.3. Monosaccharide composition analysis of PCIPS3

The monosaccharide composition of PCIPS3 was determined by high-performance liquid chromatography (HPLC) according to 1-phenyl-3-methyl-5-pyrazolone (PMP) derivatization procedures with some modification (Lv et al., 2009). Briefly, 3 mg of PCIPS3 was dissolved in 1 mL of 4 mol/L trifluoroacetic acid (TFA) in a sealed tube and hydrolyzed for 6 h at 121 °C. The excess TFA was removed with 200 μL methanol under a reduced pressure after the complete hydrolyzation. Then the dried hydrolysate of PCIPS3 or 100 μL of standard monosaccharides (2 mmol/L) were mixed with 100 μL of 0.6 mol/L aqueous NaOH and 100 μL of 0.5 mol/L PMP in methanol solution. The mixture was subsequently neutralized with 0.5 mol/L hydrochloric acid after cooling to room temperature. The resulting solution was successively extracted with the same volume of water and chloroform for three times. The aqueous layer was finally filtered through 0.45 μm pore membrane for HPLC analysis.

Analysis of the PMP-labeled monosaccharides was operated on a Dionex Ultimate3000 HPLC system (Sunnyvale, USA) equipped with a UV 6999 detector (Sunnyvale, USA). The analytical column used was a Zorbax Eclipse XDB-C18 column (4.6 mm × 250 mm, 5 μm, Agilent, USA). The wavelength of UV detection used was 245 nm. The process was carried out at a flow rate of 1.0 mL/min at 25 °C for 40 min, in which the eluent consisted of the mobile phase A (acetonitrile) and the mobile phase B (0.05 mol/L sodium phosphate (KH_2PO_4-NaOH, pH 6.9) buffer) in a ratio of 17:83. The injection volume was 10 μL.

2.4. FT-IR spectroscopy of PCIPS3

2 mg of dried PCIPS3 was mixed with 200 mg spectroscopic-grade potassium bromide (KBr) powder and pressed into 1 mm thick pellet for FT-IR spectroscopy. FT-IR spectra were recorded on a Nexus IS10 FT-IR spectrometer (Thermo Nicolet, USA) at the frequency range of 4000–400 cm^{-1} with resolution of 4 cm^{-1} and 64 numbers of scans.

2.5. Methylation analysis of PCIPS3

The determination of the linkage types of PCIPS3 was performed by methylation analysis according to the method of Ciucanu and Kerek (1984) with some slight modification. Briefly, freeze-dried PCIPS3 (4 mg) was dissolved in 0.6 mL of anhydrous DMSO (dimethylsulfoxide) and then methylated with adding 0.6 mL of cold CH_3I dropwise and 0.6 mL of NaOH-DMSO solution. After 30 min of reaction under the ultrasonic bath, the solution was extracted by 3 mL chloroform. The organic phase was washed with 6 mL distilled water before being evaporated to dryness. The disappearance of the O–H band (3200–3700 cm^{-1}) in the IR spectrum was used to confirm complete methylation. After successive hydrolysis with 3 mL of 90% aqueous formic acid for 3 h and 2 mol/L trifluoroacetic acid (4 mL) for 6 h at 100 °C, the permethylated sample was converted into partially methylated alditol acetates (PMAAs) and analyzed by gas chromatography–mass spectrometer (GC–MS). The methylation GC–MS program was carried out on Agilent 7890A/5975C instrument with a HP-5MS column (30 m × 0.25 mm × 0.5 mm) (Thermo Co., Austin, TX, USA) equipped with flame-ionization detector. The temperature was increased from 150 to 250 °C at a rate of 6 °C/min then maintained at 250 °C for 15 min. The injector and the detector temperatures were both set at 250 °C.

2.6. Partial hydrolysis with acid

Partial degradation by acid hydrolysis was subjected to elucidate the structure of branches and backbone of PCIPS3. PCIPS3 was hydrolyzed with 0.2 mol/L TFA at 100 °C for 2 h, then the excess acid was removed by evaporation. The resulting hydrolysate was dialyzed with distilled water (molecular weight cutoff 3500 Da). The retentates (the fractions in dialysis sack, PCIPS3-D1) and the dialysates (the fractions outside dialysis sack, PCIPS3-D2) were both collected and lyophilized.

2.7. NMR spectra

PCIPS3 and PCIPS3-D1 were dried for 48 h in a vacuum dryer with P_2O_5 and exchanged with deuterium by lyophilizing for three times, and finally dissolved in 0.5 mL D_2O at room temperature before starting the NMR experiments. Chemical shifts were referenced to internal 4,4-dimethyl-4-silapentane-1-sulfonic acid (^1H and ^{13}C at 0.00 ppm). The ^1H NMR, ^{13}C NMR, ^1H–^1H correlation spectroscopy (COSY), Total correlation spectroscopy (TOCSY), heteronuclear multiple quantum coherence (HMQC), heteronuclear multiple bond correlation (HMBC) and nuclear overhauser effect spectroscopy (NOESY) were recorded on a Bruker AVANCE 600 MHz spectrometer (Bruker Group, Fäl-landen, Switzerland) at 333.15 K with a Bruker 5 mm ^1H–$^{19}F/^{15}N$–^{31}P TXI switchable broadband probe. All the data was processed and analyzed using standard Bruker Topspin-NMR software (Smallcombe, Patt, & Keifer, 1995).

2.8. Chain conformation of PCIPS3

The solubilized PCIPS3 chains were characterized by size-exclusion chromatography (SEC column, TSK $G3000_{PW}$ column, 7.8 mm × 300 mm) combined with multiangle-laser photometer (DAWN HELEOS II, Wyatt Technology, USA), a degasser (GASTORR TG-14, Gen Tech Scientific Inc., USA), a pump (S-1500, SSI, USA) and a sampler (High-Pressure Injection system, Wyatt Technology, USA). A differential viscometer (ViscoStar™ II, Wyatt Technology, USA) and a refractive index detector (RID-10A, Shimazu Corporation, Japan) were simultaneously connected as well. The eluent was 0.1 mol/L aqueous $NaNO_3$ (containing 0.02% NaN_3) with a flow rate of 0.5 mL/min. The PCIPS3 sample was prepared with 0.1 mol/L $NaNO_3$ to be a concentration of 3 mg/mL and kept stirring for at least 24 h. Then all the samples were filtered on a 0.22 μm pore membrane before the injection in order to eliminate large aggregates. The refractive index increment (*dn/dc*) value of PCIPS3 in 0.1 mol/L aqueous $NaNO_3$ solution was set to be 0.138 mL/g at 658 nm (Bednar & Hennessey, 1993). All the tests were maintained at 25 °C. ASTRA software (Version 7.1.2, Wyatt Technology) was used for data acquisition and further analysis

2.9. Atomic force microscopy of PCIPS3

The atomic force microscope used in this study was a ParkProbe XE-70 system (Park Scientific Instruments, Suwon, Korea) equipped with a Z-scanner. The experiment was performed in ambient air at room temperature and a relative humidity of 30–35%. The image process was obtained in non-contact mode using a classical silicon cantilever (Si_3N_4) with a spring constant of 26 N/m and a resonance frequency of approximately 300 kHz. PCIPS3 was initially dissolved in Milli-Q water at a concentration of 1 mg/mL with continuous stirred for 2 h and incubated at 80 °C for 2 h. Then the solution was diluted to a concentration of 20 μg/mL and 10 ng/mL, successively. After filtered through a 0.22 μm filter, 2.5 μL of sample solution was dropped onto freshly cleaved mica substrate and dried in desiccator before imaging. The scan area was set at 5 μm^2, while the resolution was 512 × 512 points. The scanning linear velocity was 0.8 Hz. XEI data processing software (Version 4.3.0, Park Systems Corporation, Korea) was used for image manipulation.

2.10. Antioxidant activities in vitro

2.10.1. DPPH scavenging activity

The DPPH scavenging ability of sample was determined by the method of Chen, Xie, Nie, Li, and Wang (2008) with some modifications. Briefly, fifty microliters of PCIPS3 solutions (0.1, 0.2, 0.4, 0.6, 0.8, 1.0 and 1.2 mg/mL) were mixed with 2.5 mL of DPPH solution (0.2 mmol/L DPPH in 95% ethanol). Then, the mixtures were incubated at room temperature in the dark for 30 min, and the discolorations were measured at 517 nm. Ascorbic acid as a standard was used to be compared with the samples. Triplicate measurements were carried out for each sample. The inhibition percentage of DPPH scavenging capability was calculated as the following equation:

$$\text{Scavenging rate}\ (\%) = [1 - (A - A_b)/A_0) \times 100 \quad (1)$$

where A_0 was the absorbance of the mixture with sample replaced by 95% ethanol, A and A_b were the absorbances of DPPH solution with or without the tested sample.

2.10.2. Superoxide radical scavenging activity

The superoxide radical scavenging activity of sample was investigated by a slightly modified method (Liu, Ooi, & Chang, 1997). In this assay, PCIPS3 was dissolved in distilled water at 0, 0.1, 0.2, 0.4, 0.6, 0.8, 1.0 or 1.2 mg/mL. 1.0 mL of the sample solution was mixed with 3.0 mL of Tris–HCl buffer (16 mmol/L, pH 8.0) containing 1.0 mL of NADH (78 μmol/L) solution and 1.0 mL of NBT (50 μmol/L) solution. The reaction system was triggered by adding 1.0 mL of PMS (10 μmol/L, pH 8.0) solution and incubated at 25 °C for 5 min. Finally, the absorbance was measured at 560 nm against blank sample. Ascorbic acid was used as the reference compound. All the measurements were carried out in triplicate. The scavenging effect of the superoxide radical was defined as:

$$\text{Scavenging effect}\ (\%) = (1 - A_s/A_0) \times 100 \quad (2)$$

where A_s was the absorbance of sample and A_0 was the blank control solution without the sample.

2.10.3. Hydroxyl radical scavenging activity

The hydroxyl radical system generated by the Fenton reaction was evaluated *in vitro* according to the method described by Zhong, Lin, Wang, and Zhou (2012). Briefly, PCIPS3 of various concentrations (0, 0.1, 0.2, 0.4, 0.6, 0.8, 1.0 or 1.2 mg/mL) were mixed with 2.0 mL of $FeSO_4$ (6 mmol/L) solution and 2.0 mL H_2O_2 (6 mmol/L) solution. After thoroughly shaken, the mixture was left standing at room temperature for 10 min. Then the reaction was performed by adding 2.0 mL of salicylic acid (6 mmol/L) and allowed to stay at room temperature for another 10 min. The hydroxyl radical was detected by monitoring absorbance at 510 nm. Ascorbic acid was used as positive control. All experiments were performed three times, and the capability of hydroxyl radical scavenging activity was calculated using the following equation:

$$\text{Scavenging ability}\ (\%) = [1 - (A_s - A_j)/A_0] \times 100 \quad (3)$$

where A_0 was the absorbance control (water instead of sample solution), A_s was the absorbance in the presence of the sample, and A_j was the absorbance of the blank reagent (water instead of H_2O_2).

2.10.4. Oxygen radical absorbance capacity (ORAC) assay

ORAC assay was performed according to a previously reported protocol (You et al., 2013) with minor modification in a Synergy 2 Multi-Mode Microplate Reader (BioTek, Winooski, VT, USA). All of fluorescein (FL), AAPH, Trolox (antioxidant standard) and sample were prepared in 75 mmol/L phosphate buffer (pH 7.4). Briefly, the final reaction mixture was 200 μL containing 40 μL of fluorescein (3.5 nmol/L), 20 μL of sample solution (0.05 mg/mL) or 20 μL of Trolox (6.25, 12.5, 25, 40 and 50 μmol/L) and 140 μL of AAPH (12.8 mmol/L), where the FL and sample or Trolox solution were shaken and pre-incubated at 37 °C for 15 min in 96-well polystyrene black microplates before rapidly adding the AAPH solution. The fluorescence was read every 2 min for 98 min, where excitation and emission wavelengths were 485 and 538 nm, respectively. All determinations were carried out in triplicate. ORAC value was expressed as Trolox equivalents (μmol Trolox/g).

2.11. Immunomodulatory activity of PCIPS3

2.11.1. Cell viability

A murine macrophage cell line, RAW264.7 cells were collected from Shanghai Institute of Cell Biology (Shanghai, China) and maintained in RPMI 1640 that was supplemented with 100 U/mL penicillin, 100 U/mL streptomycin and 10% fetal bovine serum. Cells were grown at 37 °C in a humidified 5% CO_2 incubator. After incubation, cell viability was determined by CCK-8 assay.

2.11.2. Immunomodulatory activity

For drug treatment experiments, the cells were inoculated into 24-well culture plates at 3×10^5 cells per well and incubated for 24 h. The medium was then incubated with 6.25–100 μg/mL of PCIPS3 or 1 μg/mL of lipopolysaccharide (LPS) and incubated for 24 h. 10 μg/mL of Polymyxin B was also added to each well to exclude the effects of LPS, which was used as a positive reference drug in the test. Cytokines TNF-α, IL-1β, IL-6 and IL-10 in the culture supernatant were assayed with the corresponding sandwich Enzyme-Linked ImmunoSorbent Assay (ELISA) kits (eBioscience) according to manufacturer's instructions. All treatments were performed in triplicate and repeated at least once, and the results were expressed by their means ± SD (standard deviation). Statistical significance of the treatment effects was determined by Duncan's multiple range *t*-test.

3. Results and discussion

3.1. Chemical properties of PCIPS3

According to our previous work (Wei et al., 2016), the third fraction (PCIPS3) obtained from the mycelium of *P. cicadae* was separated on Sephadex G-100 gel chromatography. As shown in Fig. 1A, the profile yielded a major peak with a very small hump in the front, which could be neglected. Then the major fraction was further purified to give one symmetrical peak (Fig. 1B) through gel-filtration chromatography on Sephadex G-75. It was indicated to contain 1.78% protein using the Bradford method. Additionally, no uronic acid content was determined by photometry method at 525 nm.

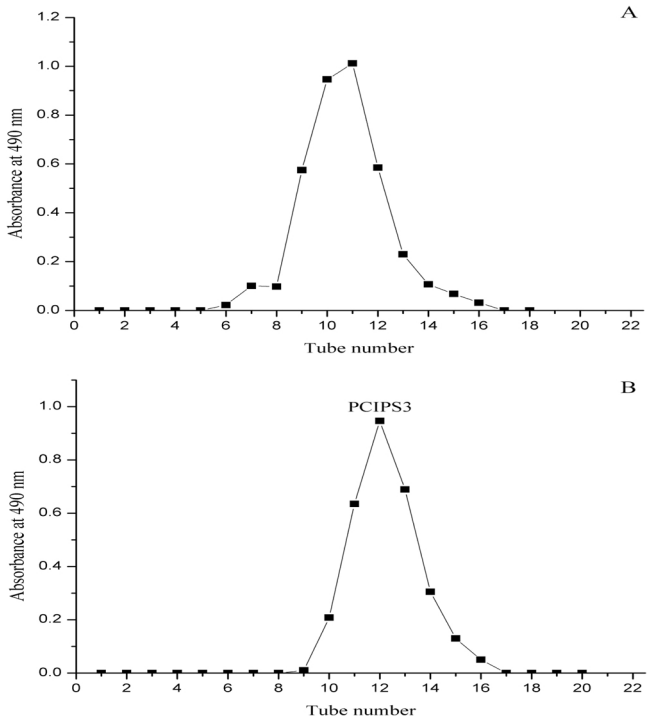

Fig. 1. The elution profile pf PCIPS3 from *P. cicadae* on Sephadex G-100 column (A) and Sephadex G-75 column (B).

Table 1
Monosaccharide compositions analysis of PCIPS3, PCIPS3-D1 and PCIPS3-D2.

Fractions	Molar ratios		
	Glucose	Galactose	Mannose
PCIPS3	23.8	2.1	1.0
PCIPS3-D1[a]	20.0	n.d.[c]	n.d.
PCIPS3-D2[b]	3.3	1.9	1.0

[a] The retentates after dialysis of hydrolysate of PCIPS3.
[b] The dialysates after dialysis of hydrolysate of PCIPS3.
[c] Not detected.

The sugar analysis of PCIPS3 by the HPLC analysis based on pre-column PMP derivatization was shown in Table 1. The results indicated that PCIPS3 was a neutral heteropolysaccharide including glucose, galactose and mannose in a molar ratio of 23.8: 2.1: 1.0. In term of molar ratios, the predominant monosaccharide was glucose, which was extremely different from the former biomacromolecules from both the natural fruiting body of *C. cicadae* and the fermented mycelium derived from *P. cicadae*. Ukai, Matsuura, Hara, Kiho, and Hirose (1982) found that the C-3, isolated from the rod-like ascocarps of *C. cicadae* through Sephadex G-100 column, was primarily composed of mannose and galactose in a ratio of 4:3. Kiho, Miyamoto, Nagai, and Ukai (1988) pointed out that two minor polymers contained mannose and galactose in a molar ratio of 1: 0.85 for CI-P and 1:0.57 for CI-A. A neutral heteropolysaccharide named as PCIPS2 had also been reported in our previous work to consist of mannose, rhamnose, 3-O-methyl-galactose, glucose and galactose with a molar ratio of 47.9:3.1:6.4:0.9:0.8 (Wei et al., 2016). It seems that the growth environment and fermentation processes might contribute to the differences of monosaccharide composition of *C. cicadae*.

3.2. FT-IR spectrum of PCIPS3

The FT-IR spectrum (Fig. 2) of PCIPS3 exhibited typical characteristics of polysaccharide. The broad peaks around at 3411 cm^{-1} was attributed to -OH stretching vibration, and the weak absorption at 2933 cm^{-1} represented C-H stretching vibration of a CH_2 group. A symmetrical absorption signal at 1633 cm^{-1} indicated the presence of C═O groups or C = C groups vibration in the structure. The absence of absorption peaks at 1730 cm^{-1} confirmed that there was no uronic acids in PCIPS3 (Wang et al., 2015). The prominent bands between 1100 and 1000 cm^{-1} were assigned to the characteristic of C—O—C glycosidic bond vibrations and ring vibrations overlapped with C-O-H stretching vibrations of side group bounds. The characteristic

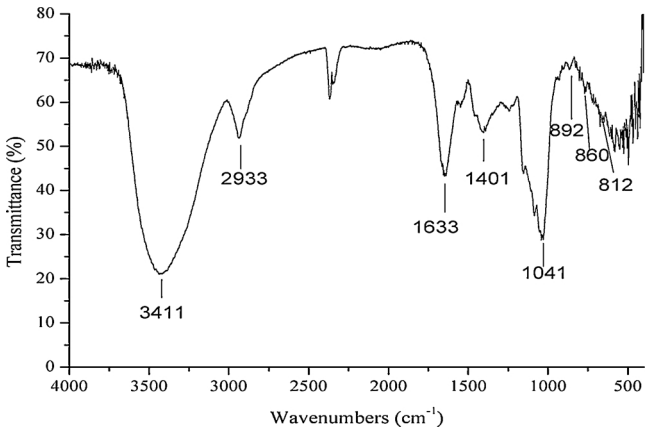

Fig. 2. IR spectrum of fraction PCIPS3 from *P.* cicadae.

Table 2
Methylation analysis of PCIPS3 and PCIPS3-D1.

Methylated sugars	Linkages[a]	Major mass fragment	Molar ratios	
			PCIPS3	PCIPS3-D1
2,3,4,6-Me_4-Glc	1-linked Glc*p*	43,71,87,102,113,118,129,145,162,205	1.35	n.d.[b]
3,4,6-Me_3-Gal	1,2-linked Gal*p*	43,71,88,101,129,145,161,190,205	0.38	n.d.
2,4,6-Me_3-Glc	1,3-linked Glc*p*	43,71,87,101,118,129,161,174,234	0.14	n.d.
2,3,6-Me_3-Man	1,4-linked Man*p*	59,71,87,102,118,129,143,162,173,203,233	0.48	n.d.
2,3,6-Me_3-Glc	1,4-linked Glc*p*	71,87,101,118,129,142,162, 173,233	10.93	10.0
2,3,4-Me_3-Glc	1,6-linked Glc*p*	43,71,87,102,113,118,129,145,162,189,233	0.27	n.d.
2,3-Me_2-Gal	1,5,6-linked Gal*f*	59,85,102,118,127,159,201, 261	1.00	n.d.

[a] Glc*p*: glucopyranose, Gal*p*: galactopyranose, Man*p*: mannopyranose, Gal*f*: galactofuranose.
[b] Not detected.

absorption peaks at 892 and 860 cm^{-1} were due to the existence of α- and β-configurations simultaneously (Zhang, Tian, Jiang, Miao, & Mu, 2014). In addition, a signal at 812 cm^{-1} suggested the presence of mannose. These results were consistent with the outcomes of HPLC analysis for PCIPS3.

3.3. Methylation analysis of PCIPS3

Methylation analysis was conducted for identification of the glycosidic linkages involved in PCIPS3. The substitution patterns of the *O*-acetyl groups on the PMAA reflected the linkage positions of the corresponding sugar residues. The PMAA prepared from PCIPS3 were analyzed through GC-MS and identified by their retention time and main characteristic ion fragments. Methylation analysis of PCIPS3 gave PMAAs corresponding to terminal Glc*p*, 2-*O*-substituted Gal*p*, 3-*O*-substituted Glc*p*, 4-*O*-substituted Man*p*, 4-*O*-substituted Glc*p*, 6-*O*-substituted Glc*p* and 5,6-Di-*O*-substituted Gal*f* (see Table 2). 4-*O*-Substituted Glc*p* accounted for around 84.4% of all residues, suggesting that the backbone of PCIPS3 may be composed mainly of (1→4)-D-glucopyranan. The presence of linkage of 5,6-linked Gal*f* indicated that PCIPS3 is a slightly branched polymer. This kind of structure was extremely different from that of PCIPS2, which had a backbone of 1,4-linked Rha*p* residues and 1,6-linked Man*p* residues instead (Wei et al., 2016). In addition, the presence of galactofuranose was evidenced by the following NMR analysis.

3.4. Partial acid hydrolysis of PCIPS3

Partial degradation of polysaccharides controlled by acid hydrolysis is on basis of the fact that glycosidic linkages in carbohydrates shows different resistance to acid treatment (Wu, Ai, Wu, & Cui, 2013). Generally, furanose is more easily hydrolyzed in dilute acid with a faster rate than pyranose. The glycosidic linkages in the side chain are more prone to be broken down than those in backbone. In this work, PCIPS3-D1 (the retentates after dialysis) and PCIPS3-D2 (the dialysates after dialysis) were obtained from partial acid hydrolysis of PCIPS3. Therefore, PCIPS3-D1 should be primarily originated from the backbone of PCIPS3. The sugar composition analysis showed that PCIPS3-D1 was exclusively composed of glucose (Table 1), implying that the backbone of PCIPS3 consisted mainly of glucopyranose. Glucose, galactose and mannose existed in PCIPS3-D2 with a ratio of 3.3:1.9:1.0 (Table 1), indicating they were presented in side chains or in furanose form. PCIPS3-D1 was also subjected to methylation analysis, and the results (Table 2) corroborated that (1→4)-D-glucopyranan might be main components of the backbone of PCIPS3. ^{1}H NMR experiments was carried out to further determine these partial hydrolysis products. By reference to proton chemical shifts of PCIPS3 (see Section 3.5), signals in ^{1}H NMR spectrum (Supplemental Fig. 1) of PCIPS3-D1 were ascribed to (1→4)-α-D-Glc*p*, α-Glc*p* and (1→4)-α-6-*O*-Me-α-Glc*p*, suggesting that 6-*O*-Me-α-Glucopyranose was also presented in (1→4)-D-glucopyranan of PCIPS3 beyond α-Glucopyranose.

3.5. NMR analysis of PCIPS3

In the ^{1}H NMR spectrum (Fig. 3A), three resonance absorptions were clearly observed at δ 5.40, 5.19 and 4.97 in the anomeric proton regions (δ 4.40–5.90). δ 5.40 containing two overlapped anomeric protons was evident from two cross resonance signals corresponding to δ 5.40 (δ 5.40/3.64 and δ 5.40/3.57) in COSY spectrum. In addition, several very weak anomeric proton peaks were found at around δ 5.23, 5.05, 4.66 and 4.64. The ^{13}C NMR spectrum (Fig. 3B) exhibited four major (δ 109.84, 102.64, 102.50 and 101.42) and several minor (δ 110.56, 107.18, 105.42, 103.38, 100.54 and 98.55) signals in the anomeric carbon regions (δ 90–112). The proton signal at δ 3.23 had a corresponding carbon signal at δ 56.85, suggesting the presence of *O*-Me. Seven residues were finally identified by a series of 2D correlation experiments (COSY, TOCSY, HSQC and HMBC) which allowed the assignment of most of the main signals of the residues in Fig. 3. To facilitate the determination of the residues, the seven anomeric carbons were labeled as A-G from high to low intensity. Those proton and carbon chemical shifts were assigned in detailed and summarized in Table 3.

For residue A, B and D, the proton resonances for H-1, H-2, H-3, H-4, H-5 and H-6 at the same system spin system were easily assigned from the correlation peaks in the TOCSY along with ^{1}H–^{1}H COSY spectra (Supplemental Figs. 2 and 3). All three residues belong to different types of glucose units according to upfield chemical shifts of H-2 (δ 3.64, 3.57, 3.59) compared to its normal position in reference. The chemical shifts of anomeric proton at δ 5.40, 5.40 and 4.97, respectively, and the small coupling constant values $J_{H\text{-}1,H\text{-}2}$ (< 3 Hz) and $J_{C\text{-}1,H\text{-}1}$ (~170 Hz) indicated that A, B and D were α-linked residues. Compared with chemical shifts of reference analogous compounds, the downfield shift of C-4 (δ 79.69) confirmed that residue A was →4)-α-D-Glc*p*-(1→ and residue B was α-Glc*p*-(1→. Two obvious inter-residual cross signals at δ 3.23/68.40 and δ 3.68/56.85 in HMBC spectrum (Fig. 3d and e) suggested that *O*-Me group was linked to residue D. The downshift resonance of C-6 at δ 68.80 and C-4 at δ 79.69 was further proved that residue D was →4)-α-6-*O*-Me-α-Glc*p*-(1→.

Likewise, residue C was of Gal-type evident from the uncompleted spin system from H-1 to H-6 and its small coupling constant between H-4 and H-5 (Staaf, Urbina, Weintraub, & Widmalm, 1999), and of β-configuration supported by the presence of the chemical shift of C-1 at δ 109.84. It was noteworthy that the clear chemical resonance of C-4 at δ 84.21 readily revealed the existence of galactofuranose unit in this residue. The chemical shifts from C-1 to C-6 for residue C corresponded nearly to the documented reference values (Parra et al., 1994), and the downfield shifts of C-5 (δ 78.34) and C-6 (δ 68.80) indicated that residue C should be designated as →5,6)-β-Gal*f*-(1→.

The proton signals of H-1, 2 and 3 for residue E were assigned from the cross peaks in TOCSY spectrum. Other proton positions were

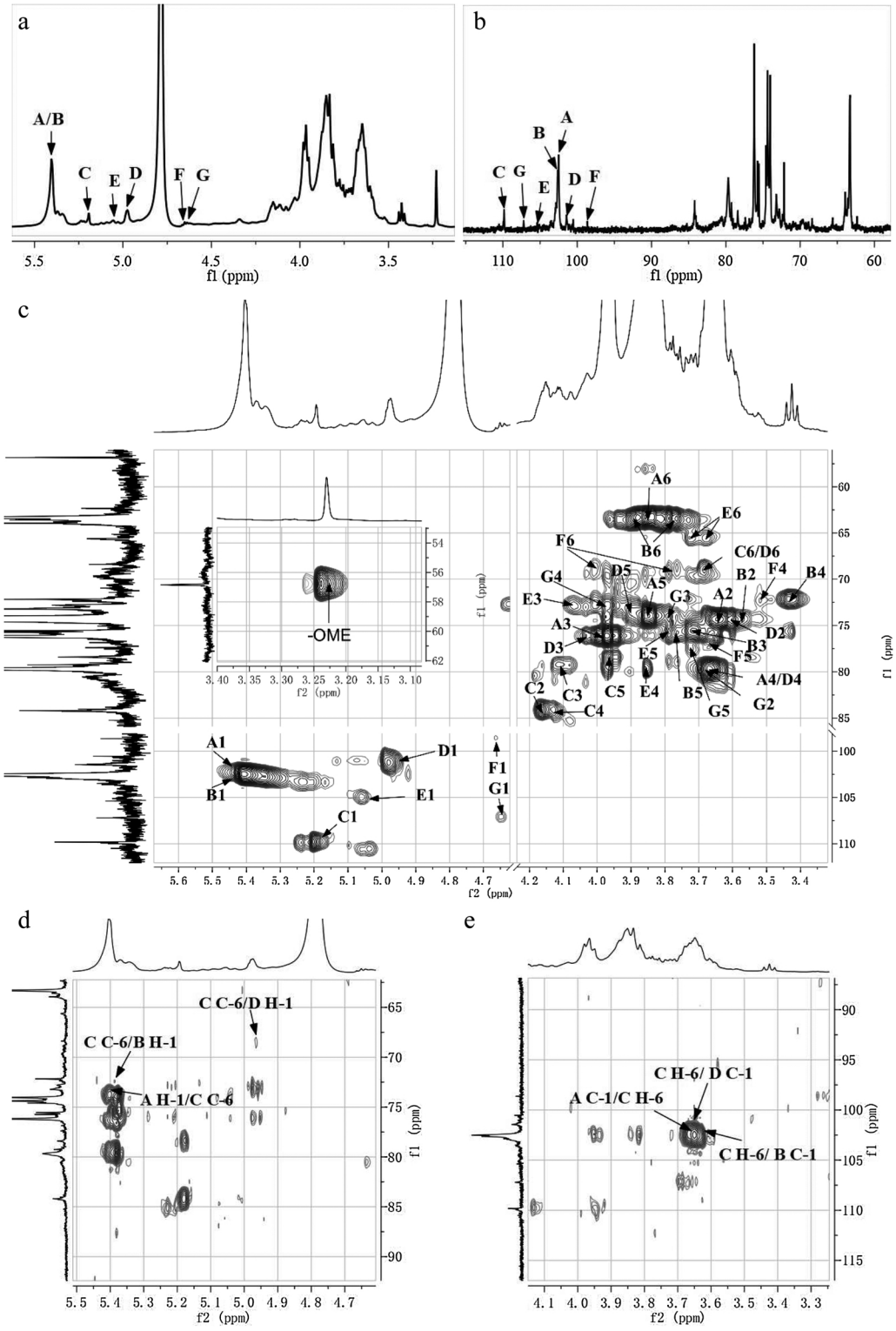

Fig. 3. NMR spectra of PCIPS3 in D_2O. (a) ^1H NMR; (b) ^{13}C NMR; (c) ^1H–^{13}C HSQC; (d and e) parts of HMBC correlation spectrum.

deduced with the combination of COSY and NOESY spectra (Supplemental Fig. 4). The correlated carbon shifts could be obtained by HSQC spectrum (Fig. 3C). With regards to the downfield shifts of H-2 (δ 4.13), C-4 (δ 79.27) and no carbon signal evident in the δ 76–82, residue E was a 1,4-disubstituted mannopyranose. In comparison with the carbon chemical signals of →4)-β-Man*p*-(1→ reported by Jansson, Lindberg, Widmalm, and Leontein (1987), residue E was undoubtedly designated as →4)-α-Man*p*-(1→.

In addition, another two anomeric proton signals could be found at δ 4.66 and 4.64 after careful identification of ^1H NMR spectrum. The other protons in the same residues were partly assigned from COSY and TOCSY spectra and corresponding carbon signals were partly provided by HSQC spectrum due to the very weak resonances. Regarding to the reference data previously reported, residue F and residue G were →6)-β-Glc*p*-(1→ and →2)-β-Gal*p*-(1→, respectively.

Both NOESY and HMBC experiments were carried out to determine

Table 3
Chemical shifts assignments of ^{1}H NMR and ^{13}C NMR spectra of PCIPS3.

Residues	H-1/C-1	H-2/C-2	H-3/C-3	H-4/C-4	H-5/C-5	H-6a,b/C-6	*O*-Me
A	5.40	3.64	3.97	**3.66**	3.85	3.85	
→4)-α-Glc*p*-(1→	102.50	74.39	76.19	**79.69**	74.04	63.28	
B	5.40	3.57	3.70	3.43	3.75	3.77, 3.86	
α-Glc*p*-(1→	102.64	74.34	75.60	72.18	75.74	63.90	
C	5.19	4.15	4.11	4.13	**3.96**	**3.68**	
→5,6)-β-Gal*f*-(1→	109.84	84.21	79.24	84.21	**78.44**	**68.80**	
D	**4.97**	3.59	4.03	**3.66**	3.91	3.68	3.23
→4)-6-*O*-Me-α-Glc*p*-(1→	**101.42**	74.34	76.26	**79.69**	73.85	68.80	56.85
E	5.05	4.13	4.08	3.85	3.77	3.68, 3.73	
→4)-α-Man*p*-(1→	105.42	–	72.81	79.27	75.88	65.50	
F	4.66	3.28	3.55	3.52	3.68	3.77, 4.00	
→6)-β-Glc*p*-(1→	98.55	76.60	78.47	72.18	77.38	68.85	
G	4.64	3.68	3.79	3.97	3.73	–	
→2)-β-Gal*p*-(1→	107.13	79.66	74.02	72.84	77.36	–	

Bold values represent glycosylation sites.

the inter/intra-linkage sequences among all the residues of PCIPS3. The cross peak δ 5.40/3.66 in NOESY spectrum implied that residue A was joined to *O*-4 of residue A or D. The strong inter-cross peaks at δ 5.40/79.69 and δ 3.66/102.50 in HMBC spectrum also implied that the backbone chain of the polymer mainly consists of (1→4)-D-glucopyranan. The inter-residual NOE correlations at δ 4.97/3.68 arising from H1 of residue D to H6 of residue C, indicated that residue D was linked to *O*-6 of residue C. The intra-residual cross signals occurring at C H-6/D C-1 (δ 3.68/101.42) and C C-6/D H-1 (δ 68.80/4.97) were attributed to residue D linked to residue C at the position of O-6. The NOE correlation at δ 5.40/3.85, δ 5.40/4.00, δ 5.40/3.68 suggested that *O*-4 of residue E, *O*-6 of residue F and *O*-2 of residue G were terminated by residue B.

Based on the monosaccharide composition analysis, the methylation results and NMR spectra (COSY, TOCSY, HSQC and HMBC), the structure character of PCIPS3 was proposed as one kind of slightly branched glucan as shown in Fig. 4. It had a main backbone consisted of 1,4-linked α-D-Glc*p* and 1,4-linked 6-*O*-Me-α-D-Glc*p* residues, which were occasionally interrupted by branched β-Gal*f* residues through 1,6-linkage. These β-Gal*f* residues were attached *via* *O*-5 position by 1,4-linked-α-Man*p*, 1,6-linked-β-Glc*p* and 1,2-linked-β-Gal*p* residues, which were terminated by α-Glc*p* residues. In this regard, PCIPS3 was similar with NCSP-50 isolated from natural *Cordyceps sinensis*, the latter was determined to have a main chain of (1→4)-linked a-D-Glc*p* (Wang et al., 2017).

3.6. Chain conformation of PCIPS3

The conformation property of PCIPS3 was investigated by using SEC combined with MALLS, viscometer and refractive index, which has been widely applied to analyze absolute molecular mass, molecular parameters and molecular morphology. The SEC-MALLS-RI-VISC chromatogram of PCIPS3, shown in Fig. 5A, reflected a single peak in the elution profile with small amounts of negligible aggregates detected by the laser light signal (LS), differential pressure (DP) signal and refractive index signal (RI) simultaneously. The M_w and the hydrodynamic radius (R_h) of PCIPS3 in 0.1 mol/L $NaNO_3$ were estimated to be 2.23×10^4 g/mol and 2.4 nm respectively. The polydispersity (M_w/M_n) of the biopolymer was 1.03, close to 1.0, indicating a homogeneous heteropolysaccharide with relatively narrow distribution of molecular weight.

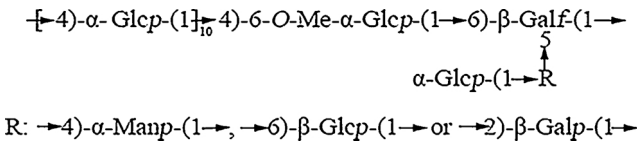

Fig. 4. Proposed structure of PCIPS3.

The relationship between intrinsic viscosity and molecular weight can be obtained by the Mark–Houwink–Sakurada (MHS) equation ($[\eta] = KM_w^{\alpha}$), where α is usually used to estimate the conformation of PCIPS3. Generally, the exponent of α lies in the range of 0.5–0.8 indicate a flexible chain in good solvent increases with a climb in chain stiffness (Burchard, 1999). The architecture information about PCIPS3 in 0.1 mol/L $NaNO_3$ solution was investigated by plotting log M_w *vs* log $[\eta]$ (Fig. 5B). After fitting the curve with linear regression, the Mark–Houwink equation was established as $[\eta] = 9.53 \times 10^{-3} M_w^{0.60}$ (mL/g). The slope ($\alpha = 0.60$) indicated that PCIPS3 existed as a flexible chain in 0.1 mol/L $NaNO_3$ aqueous solution at room temperature, which was in concert with above conclusion. Further, the molecular parameter of PCIPS3 was convinced according to the power-law function ($R_h = KM_w^{v}$) by plotting log R_h *vs* log M_w (Fig. 5C), and the exponent of v for PCIPS3 was found to be 0.53, which was in agreement with random coil conformation.

The Bushin–Bohdanecký theory is another popular method to calculate the parameters of the chain rigidity for flexible polymers by explaining the relationship between $[\eta]$ and M_w. Based on that theory, Yamakawa and Fujii (1974) later developed a worm-like cylinder model to estimate the related conformational parameters, the molar mass per unit contour length (M_L) and persistence length (q) for the stiffness of polysaccharide chain. According to the Yamakawa–Fujii–Yoshizaki (YFY) model, the $(M_w^2/[\eta])^{1/3}$ and M_w^2 could be expressed as the following equation:

$$(M_w^2/[\eta])^{1/3} = 1.516 \times 10^{-8} A_0 M_L (g^{1/3}\,cm^{-1}) + 1.516 \times 10^{-8} B_0 (2q/M_L)^{-1/2} (g^{1/3}\,cm^{-1}) M_w^2 \quad (1)$$

$$\log(d_r^2/A_0) = 0.173 + 2.158 \log d_r \quad (d_r \le 0.1) \quad (2)$$

$$d = d_r \times 2q \quad (3)$$

where the value of A_0 and B_0 depend on q and d (the hydrodynamic diameter of cylinder), and can be acquired according to the literature. Fig. 5D showed the Bohdanecký plot of PCIPS3 in 0.1 mol/L $NaNO_3$ solution, in which the intercept (45.56) and slope (3.47) could be extracted by fitting the curve with linear regression. Based on the A_0 and B_0 value, the molecular parameters of M_L, q and d for PCIPS3 were assumed as 437 nm^{-1}, 0.46 nm and 0.79 nm. These results further described that PCIPS3 adopted as a flexible chain conformation in 0.1 mol/L aqueous $NaNO_3$ solution, which was similar to a PCIPS2 with $M_L = 580\ nm^{-1}$, $q = 2.3$ nm, $d = 0.8$ nm (Wei et al., 2016).

3.7. AFM analysis of PCIPS3

AFM is an emerging technique which can overcome some limitation of methods by allowing for direct imaging of individual macromolecule

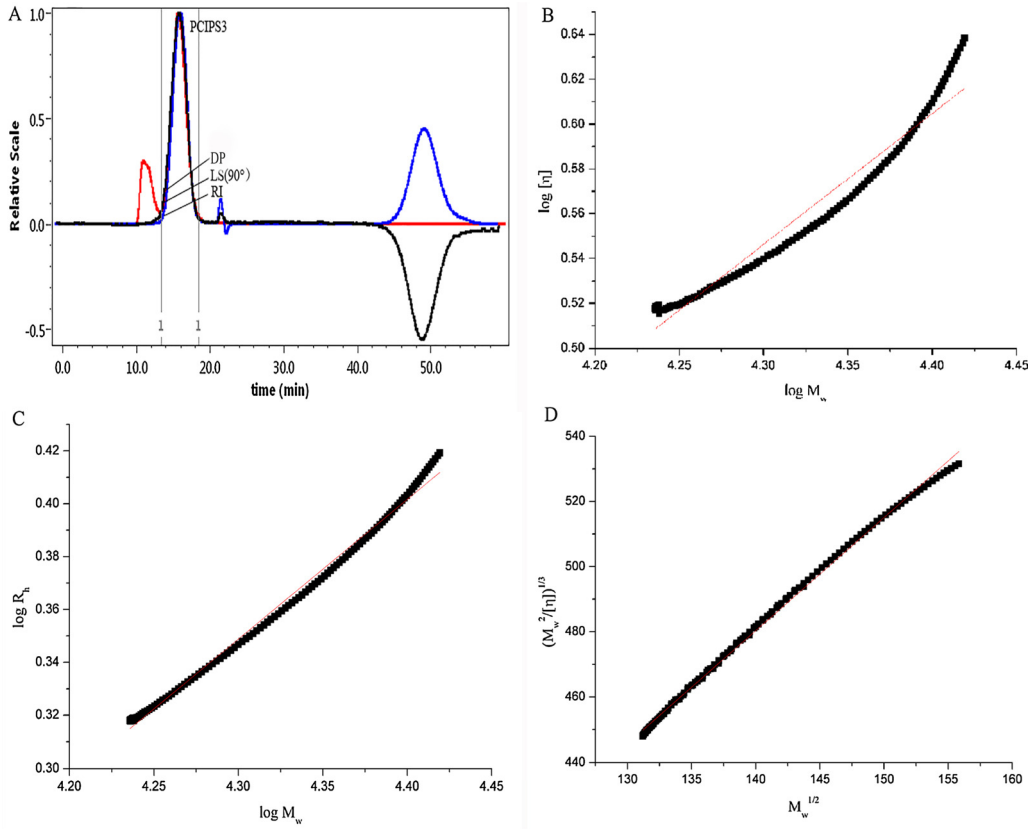

Fig. 5. SEC-MALLS-RI-VISC chromatograms of PCIPS3 (A), logarithmic plot of M_w *versus* [η] for PCIPS3 (B), logarithmic plot of M_w *versus* R_h (C) for PCIPS3 and Bohdanecký plot of $(M_w^2/[\eta])^{1/3}$ *vs* $M_w^{1/2}$ for PCIPS3 in 0.1 mol/L aqueous $NaNO_3$ solution at 25 °C (D).

at nanoscale level. Fig. 6 showed the topography of AFM for PCIPS3, which was deposited with doubly distilled water at the concentration of 20 μg/mL and 10 ng/mL. There were many small dotlike aggregates with diameters of about 150–180 nm and cross-sectional heights of approximately 0.8–1.0 nm in Fig. 6A. Those spherical-like aggregates may be entangled chains of PCIPS3 molecules in such relative low concentration solution. To achieve better continuous microfibrous and non-twined structures, the whole set of PCIPS3 was diluted into 10 ng/mL and imaged with same probe under lower-frequency scanning conditions. Fig. 6B presented a series of representative AFM images with relative discrete and flexible chains. Based on the polymer statistical analysis of an average of 50 chains, PCIPS3 were approximately 0.75 ± 0.15 nm in height and 70 nm in width. The result is consistent with the former studied chain model parameters of $M_L = 437\ nm^{-1}$, $q = 0.46$ nm, $d = 0.79$ nm. Further it confirmed that PCIPS3 exists as a flexible conformation in 0.1 mol/L $NaNO_3$ solution, which was slightly smaller and shorted than the size of PCIPS2 (Wei et al., 2016).

3.8. Antioxidant activities in vitro

3.8.1. DPPH radical-scavenging assay

DPPH is a stable N-centered free radial, which can be easily reduced by hydrogen-donating antioxidant with a rapid reduction of maximum absorbance at 517 nm. Therefore, it is commonly used as an effective and sensitive way to evaluate the antioxidant capacity of natural compounds. Fig. 7A depicts the DPPH radical scavenging power of PCIPS3. It was obvious that PCIPS3 exhibited significant scavenging ability on DPPH in a concentration-dependent manner. And the IC_{50} value of PCIPS3 was 0.28 mg/mL. There was an increase in the scavenging effect of PCIPS3 up to 0.8 mg/mL concentration (90.4%), beyond which there was no significant increase even up to 1.2 mg/mL. The results suggested that PCIPS3 had a strong scavenging effect on DPPH radical at relative low amount of addition. Similar scavenging ability has been reported on previous research. The purified exopolysaccharide (PEPS) from mycelial culture of *P. cicadae* (Miq.) Samson presented a similar scavenging ability on DPPH radical with 64.1% at a dose of 1.0 mg/mL (He et al., 2010). FPCPS obtained from the solid-state fermentation of *P. cicadae* had strong DPPH radical inhibition from dose of 0.1 to 0.6 mg/mL (Ren et al., 2014). Those data were fully consistent with the findings in this study.

3.8.2. Superoxide radical-scavenging assay

Superoxide anion, as a reduced form of molecular oxygen, could be initiated to evaluate one's antioxidant capacity due to its transformation into more reactive species, such as hydroxyl radical, singlet oxygen and hydrogen peroxide, which have been reported to induce oxidative damage in lipids, proteins and DNA (Jayakumar, Thomas, & Geraldine, 2009). In this assay, superoxide anion radicals were generated by non-enzymatic PMS-NADH system in the reduction of NBT. The scavenging activity of PCIPS3 on superoxide anion radical was shown in Fig. 7B by determination of absorbance at 560 nm. The comparison standard vitamin C showed valuable high radical scavenging activity (89.2–93.5%) in the doses from 1.0 to 1.2 mg/mL. More favorably, PCIPS3 exhibited strong power as a notable scavenger in the tested concentration range. The percentage inhibition of superoxide anion generation at 0.8 mg/mL concentration of PCIPS3 was found as 76.4%, which could bear comparison with that of FPCPS from solid-state fermented *P. cicadae* and PEPS from mycelial culture of *P. cicadae* (Ren et al., 2014; He, Wu et al., 2010). The IC_{50} value of PCIPS3 for eliminating superoxide radicals was about 0.46 mg/mL, which was slightly lower than that of W-CBP50 obtained from the fruiting bodies of cultured *Cordyceps militaris* (Chen, Wu, & Huang, 2013). W-CBP50 was characterized to have similar structure containing of α-glucose, α-mannose, α-galactose and α-arabinose with α-type glycosidic linkage.

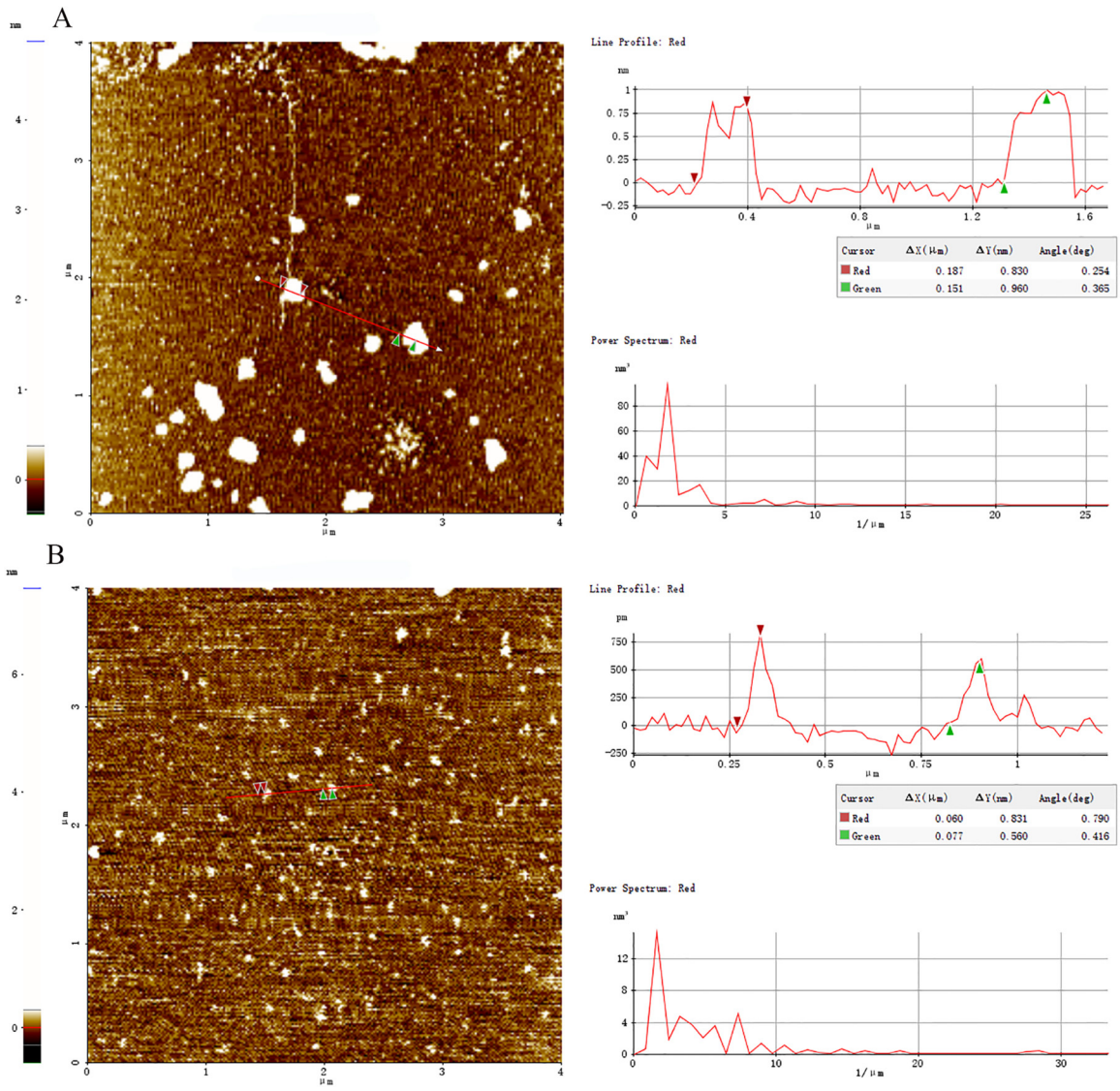

Fig. 6. Section analysis of AFM images of PCIPS3 by scan size of 4.0 nm × 4.0 nm at the concentration of 20 μg/mL (A) and 10 ng/mL (B).

3.8.3. Hydroxyl radical-scavenging assay

Hydroxyl radical is the most harmful and reactive oxygen species and is mainly responsible for the oxidative injury and lipid peroxidation. There are two types of reaction mechanism on scavenging hydroxyl radicals: one suppresses the generation of the hydroxyl radical, and the other removes the hydroxyl radicals (Tseng, Yang, & Mau, 2008). In this assay, the hydroxyl radical is generated by using Fenton's reaction of the iron (II) complex with H_2O_2 in the presence of salicylic acid. The results of hydroxyl radical scavenging activities of PCIPS3 and ascorbic acid at different concentrations were given in Fig. 7C. As illustrated in the figure, the scavenging powers of PCIPS3 and Vc both correlated well with increasing concentrations. Below the dose of 0.4 mg/mL, the inhibitory effects of Vc was markedly stronger than PCIPS3, and after that, no longer obviously increased, whereas the inhibitory effect of PCIPS3 continued to increase and was comparable to Vc at the addition concentration of 1.2 mg/mL. Within the tested concentration range, the scavenging ability of PCIPS3 was more pronounced than that of bioactive components obtained from natural and cultured *Cordyceps sinensis* (Wang et al., 2015). Although the scavenging ability of the sample was not as remarkable as that of W-CBP50, the IC_{50} value (0.32 mg/mL) of PCIPS3 was very close to those of FPCPS and PEPS (Chen et al., 2013; Ren et al., 2014; He et al., 2010). In addition, the scavenging effect of this biomacromolecule demonstrated higher capacity than those of PPM and PPE reported by Jiang, Yuan, Cai, Jiao, and Zhang (2015). PPM and PPE were both neutral heteropolysaccharides consisting of mannose, galactose, and glucose with molecular ratios of 2.99:1.00:0.34 and 38.40:1.00:1.76. Therefore, our data confirmed that PCIPS3 has potential antioxidant ability of scavenging hydroxyl radical.

3.8.4. Oxygen radical absorbing capacity (ORAC) assay

The ORAC assay was used to determine the antioxidant activity capacity of PCIPS3 against peroxyl radicals, which are the most common free radicals *in vivo* and are highly reactive and unstable. The fluorescein decay curves induced by AAPH were shown in Fig. 7D, suggesting the potent scavenging capacity for PCIPS3 (1623.44 μmol Trolox/g), which was higher than those of polysaccharides from *Laminaria japonica* (Lu, You, Lin, Zhao, & Cui, 2013) and *Polyporus umbellatus* sclerotia (He, Zhang, Zhang, Linhardt, & Sun, 2016). Normally, the antioxidant ability of polysaccharide is supposed to relate to the configuration of the sugar units and monosaccharide compositions. Concerning to its flexible chain with small branches in PCIPS3, the effect of antioxidant on peroxyl radicals scavenging was conceived to be due to its hydrogen-donating ability (Cui et al., 2016). These data suggested that PCIPS3 could be an effective electron donor capable of reacting with free radicals to convert them into more stable products.

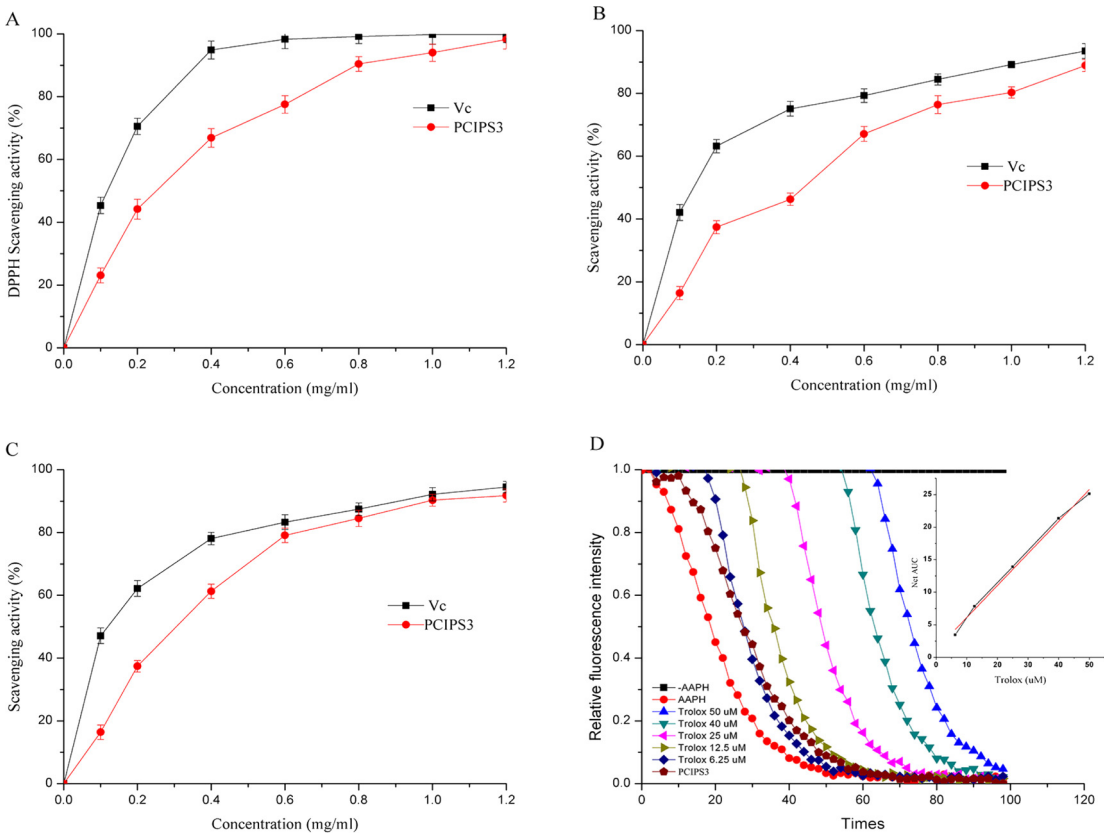

Fig. 7. Antioxidant activities of PCIPS3 from *P. cicadae* by different methods. DPPH radical scavenging assay (A); Superoxide anion scavenging assay (B); hydroxyl radical scavenging assay (C); ORAC assay (D).

3.9. Immunomodulatory activities of PCIPS3 in vitro

RAW264.7 cells are known to produce cytokines in response to the addition of LPS, and this system is usually conducted to detect the modulating activities of compounds on cytokine production (Meng et al., 2018). For investigation of the viability of RAW 264.7 macrophages, there was no significant effect of PCIPS3 on the cell viability within the range of 6.25–100 μg/mL after 24 h incubation in Fig. 8A, which indicated that the polysaccharide had no toxicity against RAW 264.7 cells *in vitro*. Three typical pro-inflammatory cytokines including TNF-α, IL-1β, IL-6 were adopted to explain the defense mechanism of macrophages against pathogens. Fig. 8B–D showed the levels of three cytokines, TNF-α, IL-1β and IL-6 in the culture medium of macrophage RAW264.7 cells after treatment with PCIPS3 and LPS. Compared with those in the control, all three cytokines were stimulated to higher levels by PCIPS3 and LPS at suitable concentrations. With regard to TNF-α, it was clear that PCIPS3 could increase the TNF-α production in a dose-dependent manner with the highest level of 318.2 pg/mL. Moreover, with respect to the other two cytokines, the secretions of IL-1β and IL-6 were significantly stimulated by PCIPS3 treatment (6.25–12.5 μg/mL, $p < 0.05$; 25–100 μg/mL, $p < 0.01$). The results suggested that PCIPS3 held a moderate potential in promoting the secretions of cytokines in RAW 264.7 cells, which further evidenced the findings made by Cheng et al., 2012. Similar phenomenon has been found in some other glucans. YCP, composed of α-D-(1–4)-linked glucose residues, interacted with TLR2 and TLR4 to induce B cells proliferation and activation (Zhu et al., 2014). Another homogenous glucan, named NCSP-50, was revealed to stimulate the proliferation of macrophages, promote nitric oxide production and enhance cytokine secretion (Wang et al., 2017). The structure of NCSP-50 closely had a backbone of α-D-(1–4)-linked glucose with terminal glucose on O-6 position.

4. Conclusion

The purified third fractionation (PCIPS3) was analyzed by HPLC, IR, methylation and 1D/2D NMR spectroscopy. The results revealed that PCIPS3 consisted of glucose, galactose and mannose in the molar ratio of 23.8: 2.1: 1.0. It had a main backbone consisted of 1,4-linked α-D-Glc*p* and 1,4-linked 6-*O*-Me-α-D-Glc*p* residues, which were occasionally interrupted by branched β-Gal*f* residues through 1,6-linkage. These β-Gal*f* residues were attached *via O*-5 position by 1,4-linked-α-Man*p*, 1,6-linked-β-Glc*p* and 1,2-linked-β-Gal*p* residues, which were terminated by α-Glc*p* residues. Moreover, the results of SEC-MALLS-RI-VISC showed that the values of M_w, R_h and $[\eta]$ for PCIPS3 were 2.23×10^4 g/mol, 2.4 nm and 9.53×10^{-3} mL/g, respectively. The α (0.60) from the Mark–Houwink–Sakurada (MHS) equation suggested that PCIPS3 adopted a flexible chain conformation with a coil-like structure in 0.1 mol/L $NaNO_3$ at 25 °C. The worm-like chains model parameters for PCIPS3 were estimated as following: $M_L = 437\ nm^{-1}$, $q = 0.46$ nm and 0.79 nm, which were further evidenced by AFM. Furthermore, PCIPS3 showed excellent scavenging capacities of DPPH radical ($IC_{50} = 0.28$ mg/mL), superoxide radical ($IC_{50} = 0.46$ mg/mL), hydroxyl radical ($IC_{50} = 0.32$ mg/mL) and ORAC radical (1623.44 μmol Trolox/g). In addition, it exhibited a moderate immunomodulatory activity by enhancing the secretion of major inflammatory cytokines in macrophages such as TNF-α, IL-1β, IL-6. These results suggested that PCIPS3 could be developed as an immunomodulator for functional foods and medicines.

Acknowledgements

We gratefully acknowledge the financial grants from the National Natural Science Foundation of China (No. 31571795), the National Natural Science Foundation of China (No. 31501815), the project of

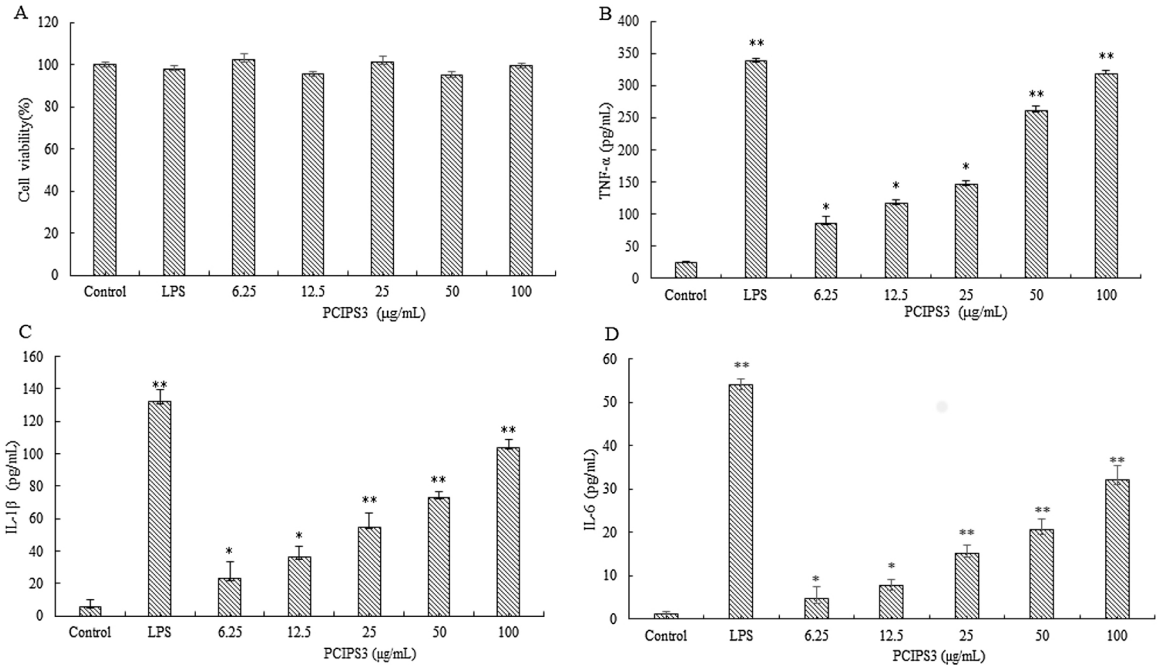

Fig. 8. Effects of PCIPS3 on the RAW 264.7 macrophages. (A) The cell viability, (B) production of TNF-α, (C) production of IL-1β, and (D) production of IL-6. Lipopolysaccharides (LPS, 1 μg/mL) were used as a positive control. Results are represented as mean ± SD. $^{*}p < 0.05$, $^{**}p < 0.01$ compared with the control group, $n = 5$.

Zhejiang Science and Technology (No. 2016F30012) and the project of Zhejiang Science and Technology (No. 2016C02057-8). The authors also thank Dr. Qiang Han from North Carolina State University, Raleigh, NC, for proofreading the manuscript.

Appendix A. Supplementary data

Supplementary data associated with this article can be found, in the online version, at https://doi.org/10.1016/j.carbpol.2019.03.104.

References

Blumenkrantz, N., & Asboe-Hansen, G. (1973). A quick and specific assay for hydroxyproline. *Analytical Biochemistry, 55*, 288–291.
Bednar, B., & Hennessey, J. P. (1993). Molecular size analysis of capsular polysaccharide preparations from *Streptococcus pneumoniae*. *Carbohydrate Research, 243*, 115–130.
Burchard, W. (1999). Solution properties of branched macromolecules. *Advances in Polymer Science, 143*, 113–194.
Chai, Y. Q., Jin, Y. W., Chen, G. J., Liu, Y. G., Li, X. L., & Wang, G. E. (2007). Separation of insecticidal ingredient of *Paecilomyces cicadae* (Miquel) Samson. *Agricultural Sciences in China, 6*, 1352–1358.
Chen, X. L., Wu, G. H., & Huang, Z. L. (2013). Structural analysis and antioxidant activities of polysaccharides from cultured *Cordyceps militaris*. *International Journal of Biological Macromolecules, 58*, 18–22.
Chen, Y., Xie, M. Y., Nie, S. P., Li, C., & Wang, Y. X. (2008). Purification, composition analysis and antioxidant activity of a polysaccharide from the fruiting bodies of *Ganoderma atrum*. *Food Chemistry, 107*, 231–241.
Cheng, J. W., Wang, Y. B., He, L., Qian, H., Fu, L. Z., & Li, H. B. (2012). Optimization of fermentation process for the production of intracellular polysaccharide from *Paecilomyces cicadae* and the immuno-stimulating activity of intracellular polysaccharide. *World Journal of Microbiology and Biotechnology, 28*, 3293–3299.
Ciucanu, I., & Kerek, F. (1984). A simple and rapid method for the permethylation of carbohydrates. *Carbohydrate Research, 131*, 209–217.
Cui, C., Lu, J., Sun-Waterhouse, D., Mu, L., Sun, W., Zhao, M., et al. (2016). Polysaccharides from *Laminaria japonica*: Structural characteristics and antioxidant activity. *LWT-Food Science and Technology, 73*, 602–608.
Ding, H. H., Qian, K. Y., Goff, H. D., Wang, Q., & Cui, S. W. (2018). Structural and conformational characterization of arabinoxylans from flaxseed mucilage. *Food Chemistry, 254*, 266–271.
Dubois, M., Gilles, K., Hamilton, J., Rebers, P., & Smith, F. (1956). Colorimetric method for determination of sugars and related substances. *Analytical Chemistry, 28*, 350–356.
He, L., Wu, X. Q., Cheng, J. W., Li, H. B., & Lu, X. Y. (2010). Purification, composition analysis, and antioxidant activity of exopolysaccharides from mycelial culture of *Paecilomyces cicadae* (Miq.) Samson (Ascomycetes). *International Journal of Medicinal Mushrooms, 12*, 51–62.
He, P., Zhang, A., Zhang, F., Linhardt, R. J., & Sun, P. (2016). Structure and bioactivity of a polysaccharide containing uronic acid from *Polyporus umbellatus* sclerotia. *Carbohydrate Polymers, 152*, 222–230.
Hu, T., Huang, Q. L., Wong, K., Yang, H., Gan, J. S., & Li, Y. R. (2017). A hyperbranched β-D-glucan with compact coil conformation from *Lignosus rhinocerotis sclerotia*. *Food Chemistry, 225*, 267–275.
Jansson, P., Lindberg, B., Widmalm, G., & Leontein, K. (1987). Structural studies of the *Escherichia coli* O78 O-antigen polysaccharide. *Carbohydrate Research, 165*, 87–92.
Jayakumar, T., Thomas, P. A., & Geraldine, P. (2009). *In-vitro* antioxidant activities of an ethanolic extract of the oyster mushroom, *Pleurotus ostreatus*. *Innovative Food Science and Emerging Technologies, 10*, 228–234.
Jiang, P., Yuan, L., Cai, D. L., Jiao, L. L., & Zhang, L. P. (2015). Characterization and antioxidant activities of the polysaccharides from mycelium of *Phellinus pini* and culture medium. *Carbohydrate Polymers, 117*, 600–604.
Ke, B. J., & Lee, C. L. (2018). *Cordyceps cicadae* NTTU 868 mycelium prevents CCl4-induced hepatic fibrosis in BALB/c mice via inhibiting the expression of pro-inflammatory and pro-fibrotic cytokines. *Journal of Functional Foods, 43*, 214–223.
Kiho, T., Miyamoto, I., Nagai, K., & Ukai, S. (1988). Minor, protein-containing galactomannans from the insect-body portion of the fungal preparation Chan Hua (*Cordyceps cicadae*). *Carbohydrate Research, 181*, 207–215.
Liu, F., Ooi, V. E. C., & Chang, S. T. (1997). Free radical scavenging activity of mushroom polysaccharide extracts. *Life Science, 60*, 763–771.
Lu, J., You, L., Lin, Z., Zhao, M., & Cui, C. (2013). The antioxidant capacity of polysaccharide from *Laminaria japonica* by citric acid extraction. *International Journal of Food Science & Technology, 48*, 1352–1358.
Lv, Y., Yang, X. B., Zhao, Y., Ruan, Y., Yang, Y., & Wang, Z. Z. (2009). Separation and quantification of component monosaccharides of the tea polysaccharides from *Gynostemma pentaphyllum* by HPLC with indirect UV detection. *Food Chemistry, 112*, 742–746.
Meng, F. C., Li, Q., Qi, Y. N., He, C. W., Wang, C. M., & Zhang, Q. W. (2018). Characterization and immunoregulatory activity of two polysaccharides from the root of *Ilex asprella*. *Carbohydrate Polymers, 197*, 9–16.
Parra, E., Jiménez-Barbero, J., Bernabé, M., Leal, J. A., Prieto, A., & Gómez-Miranda, B. (1994). Structural studies of fungal cell-wall polysaccharides from two strains of *Talaromyces flavus*. *Carbohydrate Research, 251*, 315–325.
Ren, X. Y., He, L., Cheng, J. W., & Chang, J. M. (2014). Optimization of the solid-state fermentation and properties of a polysaccharide from *Paecilomyces cicadae* (Miquel) Samson and its antioxidant activities *in vitro*. *PLOS One, 9*(2), e87578.
Shen, Y., Cai, M. X., Xia, W. L., Liu, J. W., Zhang, Q. Y., Xie, H. Y., et al. (2007). FTY720, a synthetic compound from *Isaria sinclairii*, inhibits proliferation and induces apoptosis in pancreatic cancer cells. *Cancer Letters, 254*, 288–297.
Smallcombe, S. H., Patt, S. L., & Keifer, P. A. (1995). WET solvent suppression and its applications to LC NMR and high-resolution NMR spectroscopy. *Journal of Magnetic Resonance, Series A, 117*, 295–303.
Staaf, M., Urbina, F., Weintraub, A., & Widmalm, G. (1999). Structure elucidation of the O-antigenic polysaccharide from the enteroaggregative *Escherichia coli* strain 62D1. *European Journal of Biochemistry, 262*, 56–62.
Sun, Y. F., Michael, W., Wang, P., Lu, H. F., Zhao, H. X., Liu, H. T., et al. (2017). Biological characteristics, bioactive components and antineoplastic properties of sporoderm-

broken spores from wild *Cordyceps cicadae*. *Phytomedicine, 36*, 217–228.
Tseng, Y. H., Yang, J. H., & Mau, J. L. (2008). Antioxidant properties of polysaccharides from *Ganoderma tsugae*. *Food Chemistry, 107*, 732–738.
Ukai, S., Matsuura, S., Hara, C., Kiho, T., & Hirose, K. (1982). Structure of a new galactomannan from the ascocarps of *Cordyceps cicadae* Shing. *Carbohydrate Research, 101*, 109–116.
Wang, J. Q., Kan, L. J., Nie, S. P., Chen, H. H., Cui, S. W., Phillips, A. O., et al. (2015). A comparison of chemical composition, bioactive components and antioxidant activity of natural and cultured *Cordyceps sinensis*. *LWT-Food Science and Technology, 63*, 2–7.
Wang, J. Q., Nie, S. P., Cui, S. W., Wang, Z. J., Phillips, A. O., Li, Y. J., et al. (2017). Structural characterization and immunostimulatory activity of a glucan from natural *Cordyceps sinensis*. *Food Hydrocolloids, 67*, 139–147.
Wei, C. Y., Li, W. Q., Shao, S. S., He, L., Cheng, J. W., et al. (2016). Structure and chain conformation of a neutral intracellular heteropolysaccharide from mycelium of *Paecilomyces cicadae*. *Carbohydrate Polymers, 136*, 728–737.
Weng, S. W., Chou, C. J., Lin, L. C., Wsai, W. J., & Kuo, Y. C. (2002). Immunomodulatory functions of extracts from the Chinese medicinal fungus *Cordyceps cicadae*. *Journal of Ethnopharmacology, 83*, 79–85.
Wu, Y., Ai, L. Z., Wu, J. H., & Cui, S. W. (2013). Structural analysis of a pectic polysaccharide from boat-fruited sterculia seeds. *International Journal of Biological Macromolecules, 56*, 76–82.
Xiao, J. H., Chen, D. X., Xiao, Y., Liu, J. W., Liu, Z. L., Wan, W. H., et al. (2004). Optimization of submerged culture conditions for mycelial polysaccharide production in *Cordyceps pruinose*. *Process Chemistry, 39*, 2241–2247.
Xu, Z. C., Yan, X. T., Song, Z. Y., Li, W., Zhao, W. B., Ma, H. H., et al. (2018). FTY720, a synthetic compound from *Isaria sinclairii*, inhibits proliferation and induces apoptosis in pancreatic cancer cells. *International Journal of Biological Macromolecules, 117*, 610–616.
Yamakawa, H., & Fujii, M. (1974). Intrinsic viscosity of wormlike chains. Determination of the shift factor. *Macromolecules, 7*, 128–135.
Yang, L. Q., & Zhang, L. M. (2009). Chemical structural and chain conformational characterization of some bioactive polysaccharides isolated from natural sources. *Carbohydrate Polymers, 76*, 349–361.
You, L. J., Gao, Q., Feng, M. Y., Yang, B., Ren, J. Y., Gu, L. J., et al. (2013). Structural characterisation of polysaccharides from *Tricholoma matsutake* and their antioxidant and antitumour activities. *Food Chemistry, 138*, 2242–2249.
Zhang, T., Tian, Y., Jiang, B., Miao, M., & Mu, W. M. (2014). Purification, preliminary structural characterization and *in vitro* antioxidant activity of polysaccharides from *Acanthus ilicifolius*. *LWT-Food Science and Technology, 56*, 9–14.
Zhang, Y., Wu, Y. T., Zheng, W., Han, X. X., Jiang, Y. H., Hu, P. L., et al. (2017). The antibacterial activity and antibacterial mechanism of a polysaccharide from *Cordyceps cicadae*. *Journal of Functional Foods, 38*, 273–279.
Zhong, K., Lin, W. J., Wang, Q., & Zhou, S. M. (2012). Extraction and radicals scavenging activity of polysaccharides with microwave extraction from mung bean hulls. *International Journal of Biological Macromolecules, 51*, 612–617.
Zhu, R., Zhang, X., Liu, W., Zhou, Y., Ding, R., & Yao, W. B. (2014). Preparation and immunomodulating activities of a library of low-molecular-weight α-glucans. *Carbohydrate Polymers, 111*, 744–752.